Chemical Engineering Journal 478 (2023) 147479

Contents lists available at ScienceDirect

Chemical Engineering Journal

journal homepage: www.elsevier.com/locate/cej

Intensifying levulinic acid hydrogenation using mechanochemically prepared copper on manganese oxide catalysts

Nayan Jyoti Mazumdar [a], Praveen Kumar [b,c], Miryam Arredondo-Arechavala [b], Nancy Artioli [a,d], Haresh Manyar [a,*]

[a] School of Chemistry and Chemical Engineering, Queen's University Belfast, David-Keir Building, Stranmillis Road, Belfast BT9 5AG, UK
[b] School of Maths and Physics, Queen's University Belfast, BT7 1NN, UK
[c] Shared Instrumentation Facility, Colorado School of Mines, Golden, CO, United States
[d] Department of Civil, Environmental, Architectural Engineering and Mathematics University of Brescia, Via Branze, 43, 25123 Brescia, Italy

ARTICLE INFO

Keywords:
Ball-milling
Mechanochemistry
Copper nanoparticles
Manganese oxide
Levulinic acid hydrogenation
γ-Valerolactone

ABSTRACT

A series of copper nanoparticles supported on manganese oxide octahedral molecular sieves (OMS-2) were prepared using mechanochemical (Ball-Mill) and conventional wet-impregnation (Wet-Imp) methods. All catalysts prepared were thoroughly characterized using ICP-OES elemental analysis, X-ray diffraction (XRD), N_2 sorption, H_2 temperature programmed reduction (TPR) and transmission electron microscopy (TEM) techniques. The catalyst preparation methods greatly affected the size of the Cu nanoparticles. TEM images showed that 5 wt % Cu/OMS-2 (Ball-Mill) catalyst had a narrow particle size distribution with an average Cu nanoparticle size of 2.1 nm, while the corresponding 5 wt% Cu/OMS-2 catalyst prepared using wet-impregnation method had an average Cu nanoparticle size of 19.2 nm. The structural features of the catalysts were corelated with the catalytic activity using the liquid phase hydrogenation of levulinic acid (LA) to γ-valerolactone (GVL), as an exemplar process. In LA hydrogenation at 190 °C and 20 bar H_2 pressure, the ball milled catalysts achieved higher LA conversion, and greater GVL yield, as compared to the corresponding catalysts prepared by wet-impregnation method, reinforcing that Cu nanoparticle size and metal dispersion are important tool to intensify the catalytic activity. For instance, 5 wt% Cu/OMS-2 (Ball-Mill) catalyst achieved almost twice the turnover frequency (TOF), 24.7 h^{-1} as compared to the 5 wt% Cu/OMS-2 (Wet-Imp) catalyst, TOF 11.8 h^{-1}, under identical reaction conditions. The results of this study demonstrate that ball milling is a superior method for Cu/OMS-2 catalyst preparation than wet impregnation.

1. Introduction

Sustainable development prerequisites the use of biomass-derived feedstocks, platform chemical processes with minimal waste generation, and the use of earth-abundant metals in heterogeneous catalysts. To achieve this, mechanochemical synthesis of catalysts offers a promising approach, as it enables a straightforward and waste-free method for catalyst preparation [1]. Mechanochemistry is an attractive alternative to traditional synthesis methods due to its environment friendly and economically efficient nature. It is less developed compared to traditional metal impregnation techniques like incipient wetness, wet impregnation, and coprecipitation. It offers several advantages, including the absence of solvents and washing waste. Fewer synthesis steps make it an effective method for preparing catalysts, as shown by numerous studies demonstrating the production of high-performance catalysts with excellent selectivity and activity. Additionally, decrease in particle size with the help of mechanochemical synthesis can increase the surface area, which can also contribute to an improvement in catalytic activity [2]. For example, in our recent study, Pt-Re/TiO_2 catalysts prepared by ball milling exhibited significantly higher selectivity towards the desired alcohol product (89 %) compared to conventionally prepared catalysts (69 %) in the selective hydrogenation of stearic acid. Monometallic mechanochemically prepared Pt/TiO_2 catalyst produced stearyl alcohol in 100 % selectivity, higher than conventionally prepared catalyst at the same conversion [3]. The current focus on sustainability and achieving net-zero emissions has made mechanochemistry research increasingly important. Catalyst preparation methods range from simple grinding with a mortar and pestle to

* Corresponding author.
E-mail address: h.manyar@qub.ac.uk (H. Manyar).

https://doi.org/10.1016/j.cej.2023.147479
Received 10 July 2023; Received in revised form 12 October 2023; Accepted 15 November 2023
Available online 17 November 2023

more sophisticated ball mills, which can be used on both laboratory and commercial scales. The solvent-free conditions and direct preparation of catalysts from metal oxides reduce the environmental impact. In this study, we prepared various Cu nanoparticles supported on manganese oxide octahedral molecular sieves (OMS-2) catalysts, both conventionally using cupric nitrate ($Cu(NO_3)_2{\cdot}2.5H_2O$) and mechanochemically using copper oxide (CuO) as precursors, and evaluated using liquid phase hydrogenation of levulinic acid (LA) to γ-valerolactone (GVL), as an exemplar tool (Scheme 1), to compare the catalytic activity and structural features of the catalysts prepared.

Liquid phase catalytic hydrogenation is a flexible and widely used process with applications in numerous industries such as fine chemicals, agrochemicals, and lubricants [4–6]. This process is also applicable for direct conversion of organic acids derived from biomass, such as LA, to high-value cyclic esters, such as γ-valerolactone (GVL). The cyclic esters, such as GVL, are characterised by a ring structure comprising a carbonyl group (C = O) and an oxygen atom. They are mostly used in the production of solvents, chemicals, flavours, fragrances, and are increasingly being investigated for application in biofuels, chemical intermediates, and pharmaceuticals [7]. The esters market (including GVL) is predicted to grow at a compound annual growth rate (CAGR) of 2.24 % through the forecast period, with a projected market size of USD 801.99 million by 2028 [8]. GVL can be synthesized by subjecting LA to an acid-catalysed dehydration process to form α-angelica lactone (AL), which is then hydrogenated to form GVL [9–11]. A catalyst with a well-balanced ratio of metal and acidic sites is essential for achieving high efficiency during both the dehydration and hydrogenation processes. It typically involves harsh reaction conditions such as high temperatures up to 250 °C and H_2 pressure > 25 atm. [12–15]. The use of noble metal catalysts such as iridium (Ir), ruthenium (Ru), nickel (Ni), platinum (Pt), gold (Au), and palladium (Pd) has been explored to produce GVL from LA [16–19]. The high cost associated with noble metals limits their applicability on an industrial scale. Hence, there is an urgent need to develop efficient hydrogenation catalysts consisting of low cost, earth-abundant non-noble metals.

Copper is a non-noble metal that holds promise as a potential alternative catalyst for this purpose [20]. However, harsh reaction conditions are still required, for example: Cu/ZrO_2 (200 °C, 35 bar H_2), $Cu\text{-}WO_3/ZrO_2$ (200 °C, 50 bar H_2), $Cu\text{-}Ni/\gamma\text{-}Al_2O_3$ (250 °C, 65 bar H_2) [17,21,22]. Various groups have reported Cu-based catalysts for the hydrogenation of LA to GVL using different oxides as supports [23–28]. Among these methods, Yuan et al. achieved an average CuO particle size of 12 nm using the oxalate-gel co-precipitation method, resulting in a 60 % LA conversion [29]. Orlowski et al. introduced the pH gradient method for preparing Cu/ZrO_2 catalysts for LA hydrogenation, yielding particles ranging from 6 to 87 nm and a 60 % GVL yield [20]. They noted an increase in the crystallite size of Cu species as the pre-reduction temperature of the catalysts increased. Yu et al. developed Cu-Ni bimetallic catalysts with an average particle size of 9.52 nm using the co-impregnation method [30]. The addition of acidic sites, specifically Al, in a 1:1 ratio significantly increased the GVL yield. Employing high-surface-area supports like Al_2O_3, which provided high metal dispersion, Cai et al. prepared $Cu\text{-}Ni/Al_2O_3$ catalysts with an average particle size of 6–7 nm through the incipient impregnation method, resulting in a 97 % GVL yield [31]. Hengne et al. obtained Cu particle sizes of 10–14 nm via the co-precipitation method [21]. They determined the Cu particle size to be 13.5 nm with over 90 % selectivity to GVL, further noting that the Cu particle size increased to 15 nm, possibly due to copper agglomeration after the reaction. Fang et al. prepared Cu-Ni nanoparticles with an average particle size of 7 nm on SBA-15 using a glycol-assisted impregnation method, leading to higher selectivity towards GVL [32]. These examples demonstrate that catalysts for LA hydrogenation to GVL are typically prepared using methods such as wet-impregnation, precipitation-deposition, and co-precipitation. Most of these techniques generate solvent waste and exhibit limited metal dispersion. The utilization of mechanochemical methods for developing Cu catalysts of this nature has been relatively unexplored. To our knowledge, this is the first report using mechanochemical preparation for synthesis of very small Cu nanoparticle catalysts with average Cu NP size of < 5 nm. In the prior art in literature, using wet chemical methods such as impregnation or precipitation, Cu NPs in the range of 5–85 nm have been reported. In our study, using ball-milling, it is possible to achieve very small Cu nanoparticles (average particle size 2.1 nm) with high Cu metal dispersion. For sustainable manufacturing, it is essential to increase our reliance on the use of earth-abundant metals such as Cu instead of precious metals such as Pt, Pd or Ru, routinely employed in hydrogenation reactions. The application of mechanochemistry in solid catalyst preparation offers significant advantages due to its speed, simplicity, and environment friendly solvent-free conditions [33].

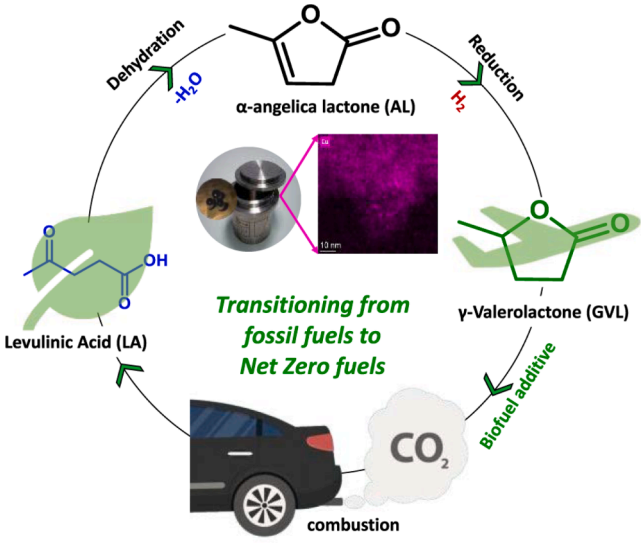

Scheme 1. Reaction pathway for the hydrogenation of LA to GVL.

Mechanochemical synthesis has emerged as a promising method for preparing efficient catalysts, as it allows for better metal dispersion on the support, resulting in higher catalytic activity and energy efficiency and offers the advantage of reduced solvent waste compared to conventional techniques. Additionally, this method can achieve increased reaction rates at lower temperatures than those required for conventional processes [34,35]. Notably, the activity of the catalysts was found to be linked to the length of the grinding time, which enhances metal dispersion, decreases particle size, and increases surface area [36]. One potential strategy, which we are adopting in our research group, for designing superior Cu nanoparticle catalysts with better activity is achieving smaller nanoparticle size and strong Cu-support interactions, which promote metal dispersion, in particular at high Cu loading. In our earlier studies, OMS-2 materials have been shown to be efficient in a wide array of reactions involving hydrogenation, oxidation and decomposition [37,38]. Manganese oxides with tunnel structures, doped with Pd on their surfaces were used effectively to remove soot, where O_2 vacancies in lattice promoted soot oxidation, which occurs over Mars-van Krevelen mechanism [39–41]. We established the efficiency of metal-doped OMS-2 as selective catalysts for reducing cinnamaldehyde to cinnamyl alcohol [42,43]. OMS-2 was found to be an effective and selective catalyst for hydrogenation, with Pt-doping improving the reaction by increasing H_2 dissociation [44–46]. We have also shown the hydrogenation of LA using a series of Cu/OMS-2 catalysts prepared through conventional methods, under optimized reaction conditions (190 °C, 20 bar H_2) [47]. The average size of Cu nanoparticles was found to be 26 nm, which were mostly spherical and elongated shapes. However, to improve the catalyst activity more comprehensively, it is required to achieve smaller Cu nanoparticle size through changes in the catalyst preparation method. This approach can provide a superior and

more efficient catalysts, leading towards sustainable catalysts using earth abundant non-noble metals.

In continuation of our group's interest in environmental catalysis [48–54], in this work, we compare the structural features and catalytic activity of mechanochemically prepared Cu on manganese oxide catalysts with corresponding Cu catalysts prepared using conventional wet-impregnation method, using liquid phase hydrogenation of LA to GVL, as an exemplar process. Our aim was to understand the impact of catalyst preparation method on the Cu nanoparticle size and how they influenced the catalytic activity and corresponding turnover frequency (TOF) values in the liquid phase hydrogenation of LA to GVL.

2. Experimental section

2.1. Materials

The chemicals used in this study were obtained from various sources and used without further purification. Levulinic acid ($C_5H_8O_3$, 98 % purity), copper nitrate hemi-pentahydrate ($(Cu(NO_3)_2{\cdot}2.5H_2O$, 98 % purity) were purchased from Alfa Aesar. Copper (II) oxide (CuO, ≥99.0 % purity) and 1,4-dioxane ($C_4H_8O_2$, 99 % purity) were also obtained from Alfa Aesar. γ-valerolactone ($C_5H_8O_2$, 99 % purity), α-angelica lactone ($C_5H_6O_2$, 98 % purity), tetrahydrofuran ($(CH_2)_4O$, 98 % purity), and maleic acid ($C_4H_4O_4$, 98 % purity) were purchased from Sigma Aldrich. Potassium permanganate ($KMnO_4$, 98 % purity) was procured from Honeywell Fluka.

2.2. Catalyst preparation

2.2.1. Synthesis of OMS-2

OMS-2 was synthesized using a modified sol–gel method, as reported in our previous work [47]. Typically, a measured amount of $KMnO_4$ was added in deionised water and stirred for 1 h. Maleic acid was slowly added to this solution in the molar ratio of 3:1, and the solution was further stirred for 3 h at room temperature. A dark brown gel was formed on the top layer which was allowed to settle and then decanted off. Deionised water was added, and the solution was stirred again for 10 mins and the process was repeated three times. The resultant mixture was vacuum filtered to separate excess water and dried overnight in the oven at 120 °C. The dried OMS-2 was calcined at 450 °C for 3 h in presence of air.

2.2.2. Synthesis of Cu/OMS-2 catalysts by wet-impregnation

A range of Cu/OMS-2 catalysts with varying wt.% of Cu were prepared using the conventional wet-impregnation (Wet-Imp) method. Initially, a fixed amount of $Cu(NO_3)_2{\cdot}2.5H_2O$ was dissolved in H_2O and stirred for 25 mins. OMS-2 was slowly added to the solution, and the mixture was agitated at 450 rpm at room temperature for another 3 h. The temperature was then increased to 70 °C, and the subsequent slurry was dried overnight at 110 °C in an oven. The sample was then calcined at 550 °C for 6 h. Catalyst abbreviations are as follows: 5 wt% Cu/OMS-2 (Wet-Imp) – 5 wt% Cu loaded catalyst prepared by conventional wet-impregnation; 10 wt% Cu/OMS-2 (Wet-Imp) – 10 wt% Cu loaded catalyst prepared by conventional wet-impregnation; 20 wt% Cu/OMS-2 (Wet-Imp) – 20 wt% Cu loaded catalyst prepared by conventional wet-impregnation.

2.2.3. Synthesis of Cu/OMS-2 catalysts by mechanochemical method

All the catalysts were prepared using the Retsch PM 100 planetary ball mill. Catalyst abbreviations are as follows: 5 wt% Cu/OMS-2 (Ball-Mill) – 5 wt% Cu loaded catalyst prepared mechanochemically; 10 wt% Cu/OMS-2 (Ball-Mill) – 10 wt% Cu loaded catalyst prepared mechanochemically; 20 wt% Cu/OMS-2 (Ball-Mill) – 20 wt% Cu loaded catalyst prepared mechanochemically. For example: to synthesize 5 wt% Cu/OMS-2 (Ball-Mill), 0.12 g of CuO as the copper precursor and 1.9 g of OMS-2 were placed into a 125 ml agate grinding jar with three balls (20 mm Ø). Milling was conducted at a speed of 150 rpm for 1 h. After completion of milling, the resulting solid powders were collected and calcined at 450 °C for 3 h in presence of air.

2.3. Catalyst characterisation

Powder X-ray diffraction (XRD) analysis was carried out using a PANalytical X'PERT PRO MPD diffractometer, equipped with a nickel filter, and operated at 40 kV and 40 mA with CuKα radiation (1.5405 Å). The measurements were taken from 5 to 90 degrees (2θ) with a counting time of 0.5 s. Scherrer equation was applied to determine the mean size of Cu NPs.

$d = \frac{0.9\lambda}{\beta cos\theta}$ where d is the mean diameter of Cu NPs (nm), λ is the wavelength of the X-ray radiation source (nm), β is the full width at half maximum (FWHM, radians) of the peak at the given diffraction angle, 2θ.

To determine the surface areas, pore volumes, and average pore diameters of the catalysts, N_2 adsorption–desorption isotherms at 77 K were measured using a Micromeritics ASAP 2020 instrument. The Brunauer-Emmett-Teller (BET) equation was used for surface area analysis, and Barrett-Joyner-Helenda (BJH) model was used for pore volume analysis. The percentage of metal loading was determined by analysing the Cu content of the catalysts using Perkin-Elmer Optima 4300 ICP-OES instrument. The reducibility of the catalysts, H_2 temperature-programmed reduction (H_2-TPR) analysis was conducted using a Micromeritics AutoChem II instrument. The samples (0.1 g) were loaded in a quartz U-tube and heated under 10 % H_2-Ar from room temperature to 800 °C at a heating rate of 15 °C min^{-1}. Cu surface area (m^2 g_{Cu}^{-1}) were estimated using following equation, by assuming all copper particles were spherical. Cu surface area (m^2 g_{Cu}^{-1}) = (100.mol H_2. SFactor.NA)/(Cu_{SD}.$Cu_{wt.\%}$), where mol H_2 = H_2 consumed/unit mass of catalyst (mol H_2/g_{cat}); SFactor = stoichiometric factor = 1; N_A = Avogadro's No. = 6.022 x 10^{23} atoms/mol; Cu_{SD} = Surface density of Cu = 1.47 x 10^{19} atoms/m^2; $Cu_{wt.\%}$ = Cu wt.% in catalyst (from ICP analysis).

Scanning transmission electron microscopy (STEM) was performed using a Thermo-Fisher Talos F200X G2 microscope operating at 200 kV, equipped with a FEG (field emission gun) and four in-column Super-X energy-dispersive X-ray (EDX) spectrometer detectors having a total collection angle of approximately 0.9 sr. To prevent agglomeration, the catalyst was mixed with ethanol and sonicated for 5 min prior to preparation. The resulting mixture was drop-casted onto a nickel grid for observation. The average size of Cu nanoparticles (NPs) was calculated using ImageJ software by determining > 100 particles and taking the average. All the catalysts (Wet-Imp, Ball-Mill) were examined after calcination and before being used in reaction.

2.4. Catalytic activity

The hydrogenation reaction of LA to GVL was performed in a 100 ml Autoclave Engineers' reactor with pressure and temperature limits of 200 bar and 200 °C, respectively. Initially, 200 mg of catalyst and 30 ml of 1,4-dioxane:water (3:7 mol ratio) were charged into the reactor for catalyst pre-reduction, and the residual gas was purged with H_2. The reactor was then heated to 200 °C, pressurized with 20 bar H_2, and stirred at 1500 rpm for 2 h. Following pre-reduction of the catalyst, 1 g of LA was introduced into the reactor, and the reactor was purged four times with H_2 to remove any residual gas. Subsequently, the reactor was heated to 190 °C, pressurized with 20 bar H_2, and agitated at 1500 rpm. This was considered as time zero. During the reaction, small samples were collected at specific intervals, filtered, and analysed by Perkin–Elmer Clarus 500 GC equipped with an FID detector and a Zebron ZB-Wax column (30 m, 0.32 mm, 0.25 mm). THF was used as an internal standard.

Turnover frequency, TOF (h^{-1}) was calculated using the following formula = [(moles of LA converted)/(moles of Cu x time)]

3. Results and discussions

3.1. Catalyst characterization

We have compared Cu/OMS-2 catalysts with varying Cu loading (5, 10 and 20 wt%) prepared with Wet-Imp and Ball-Mill methods. The catalysts were thoroughly characterized as shown in Table 1 using BET specific surface area ($m^2\ g^{-1}$), pore volume ($cm^3\ g^{-1}$) to understand the structural properties.

The comparison of theoretical and measured Cu loading, wt.% was performed using ICP-OES analysis. Similar Cu wt.% loadings were reached with both preparation methods. However, significant difference was observed in the structural properties, based on the catalyst preparation method. Ball-Milled catalysts showed higher BET surface area as compared to the Wet-Imp catalysts even at similar Cu wt.% loadings. The increased surface area from the Ball-Milled catalysts could be a result of the impacts between grinding balls of the ball mill, CuO and OMS-2. The pore volume of the Ball-Mill catalysts, analysed in the range of 0.11–0.14 $cm^3\ g^{-1}$ were in the same range as Wet-Imp catalysts. The X-ray diffraction analysis (Fig. 1**a**) for OMS-2 showed peaks at 2θ values 12.6°, 28.7°, 41.9°, and 60.1°, which are suggestive of the cryptomelane structure [55]. Fig. 1**a** also indicated that the Cu in the synthesised catalysts was in the form of CuO (monoclinic), with diffraction peaks at 2θ values 35.6° (0 0 2), consistent with the peaks of CuO standard obtained from the International Centre for Diffraction Data (ICDD) card (JCPDS file no. #48–1548) [56]. Cuprite (Cu_2O) diffraction peaks were also seen at angles 32.6° (1 1 0), 36.2° (1 1 1) and 42.4° (2 0 0), indicating the existence of Cu_2O in the prepared catalysts [57]. Average Cu crystallite sizes of the catalysts were estimated using Scherrer equation. For the Wet-Imp method, it was found to be 19.9, 20.9 and 21.2 nm for 5, 10 and 20 wt% Cu/OMS-2 respectively. As shown in Fig. 1**(a)**, the Cu crystallite size for both 5 wt% Cu/OMS-2 catalysts was calculated from the 2θ values of diffraction peaks 32.6°, 35.6° and 42.4° which is consistent with literature [56,57]. Fig. 1**(b)** demonstrates a comparison of all the XRD patterns of 5–20 wt% Cu/OMS-2 Wet-Imp and Ball-Mill catalysts. A distinguishing feature amongst the Wet-Imp and Ball-Mill catalysts is the intensity of the CuO diffraction peak at a 2θ value of 35.6°, which increases with higher Cu loadings. It implies the increase of the CuO crystallite size formed and is confirmed from the Scherrer equation calculation of CuO size for Wet-Imp catalysts. While we do notice a similar pattern of CuO peak in the Ball-Mill catalysts, it's essential to highlight that the overall intensity of the entire pattern is significantly lower, which suggests a greater dispersion of Cu on the support. It complements the Cu crystallite sizes using Scherrer equation for the Ball-Mill catalysts, which were found to be 3.63, 4.32, 5.31 nm for 5, 10 and 20 wt% Cu/OMS-2 respectively (Table 1).

STEM analysis of the catalysts was done to further study the morphology, particle size distribution of Cu supported on manganese oxide nanorods and is shown in the STEM-HAADF images and EDX analysis in Fig. 2. 5 wt% Cu/OMS-2 (Ball-Mill) (Fig. 2**(a)**) exhibited uniform distribution of Cu on the support. Elemental mapping of Cu (Fig. 2**(b)**) showed high dispersion of Cu on the manganese oxide nanorods, which confirms the absence of Cu diffraction peaks from Fig. 1**,** was a proper correlation to a better distribution of Cu. Fig. 2**(c)** shows the elemental mapping of manganese (Mn) in the ball-milled catalyst. In contrast, 5 wt% Cu/OMS-2 (Wet-Imp) (Fig. 2**(d)**) displayed relatively larger Cu nanoparticles on the support. The elemental mapping (Fig. 2**(e)**) showed a non-homogeneous distribution of Cu with large agglomerates of Cu and CuO on the nanorods. Fig. 2**(g)** compares a Cu-size distribution histogram of both the catalysts with an average particle size of 2.1 nm (Ball-Mill) and 19.2 nm (Wet-Imp). It clearly reveals the narrow particle size distribution of catalyst particle size (1 – 5 nm) which was achieved by ball-milling, compared to a wide range of large particle range between 11 and 25 nm with conventional wet-impregnation method.

The H_2 reduction profiles of Ball-Milled and Wet-Imp catalysts were studied using H_2-TPR analysis. Varying surface interactions between Cu and mixed metal oxide support result in different reduction patterns. As shown in Fig. 3 **(a),** the reduction peak at around 190 °C was observed for 5 wt% Cu/OMS-2 (Wet-Imp) which can be ascribed to Cu^{2+} reduction to Cu^{+} [58]. Similarly, peak around 220 °C, 320 °C for 5 wt% Cu/OMS-2 (Ball-Mill), could be attributed to the reduction of Cu^{+} to Cu^{0} and bulk CuO to Cu^{0} [59–62]. The multiple shoulder peaks at 250 °C for 5 wt % Cu/OMS-2 (Ball-Mill) can be correlated to stronger Cu-Mn oxide interaction [63]. Similar trend is also observed in 10, 20 wt% Cu/OMS-2 catalysts prepared by both Wet-Imp and Ball-Mill methods (Fig. 3 **(b)**). It also complements previous literature, where catalyst having low amount of Cu content and evenly dispersed, interact more strongly with the supporting material thereby developing strong metal support interaction (SMSI), which also inhibits the broadly dispersed copper species to form large Cu agglomerates under the reducing environment [64]. Reduction of the support OMS-2 from Mn^{+4} to Mn^{+3} can also be detected in the peaks ranging from 350 to 400 °C [65].

3.2. Catalytic activity in LA hydrogenation to GVL

LA hydrogenation to GVL was performed using catalysts prepared by Wet-Imp and Ball-Mill. All the catalysts were evaluated under same conditions: 1 g of LA and 0.2 g of the catalyst in a 30 ml solvent mixture of 1,4-dioxane and H_2O (3:7 mol ratio). Reaction was completed at 190 °C and 20 bar H_2 for 240 mins. The results as shown in Fig. 4, demonstrate that Ball-Milled catalysts display higher LA conversion than the corresponding Cu wt.% Wet-Imp catalysts. The LA conversion-time profiles exhibit ~ 100 % LA conversion in 4 h with all Ball-Milled catalysts. From Fig. 4**(a)** demonstrates that 5 wt% Cu/OMS-2 (Wet-Imp) showed a lower LA conversion and required a longer reaction time to reach full conversion, as compared to 5 wt% Cu/OMS-2 (Ball-Mill). Similar trend is observed for 10, 20 wt% Cu/OMS-2 catalysts in Fig. 4**(b, c)**. The superior performance of Ball-Milled catalysts is believed to be due to the smaller Cu NPs sizes, and higher surface areas. These results implied that the Ball-Milling is a more favourable approach for making

Table 1
Structural properties of Cu/OMS-2 catalysts.

	OMS-2	5 wt%Cu/OMS-2		10 wt%Cu/OMS-2		20 wt%Cu/OMS-2	
		Wet-Imp	Ball-Mill	Wet-Imp	Ball-Mill	Wet-Imp	Ball-Mill
Cu (wt%)[a]	No Cu	5.06	5.03	10.8	10.7	20.9	20.5
BET surface area, (m^2g^{-1})[b]	76.1	27.3	33.4	23.6	38.2	20.7	32.4
Pore volume, (cm^3g^{-1})[c]	0.25	0.14	0.14	0.11	0.11	0.11	0.11
Avg. CuO crystallite size (nm)	**XRD analysis[d]**	19.9	3.63	20.9	4.32	21.2	5.31
	TEM analysis[e]	19.3	1–3	20.0	1–3	22.0	1–3
Cu surface area ($m^2\ g_{Cu}^{-1}$)	–	19.0	41.0	18.6	25.0	10.0	15.0

[a]Determined from ICP-OES measurements; [b]Determined from BET analysis; [c]Determined from BJH method; [d]Calculated from Scherrer Eqn; [e]Determined from ImageJ software.

Please check 1st figure changed as Fig. 2.

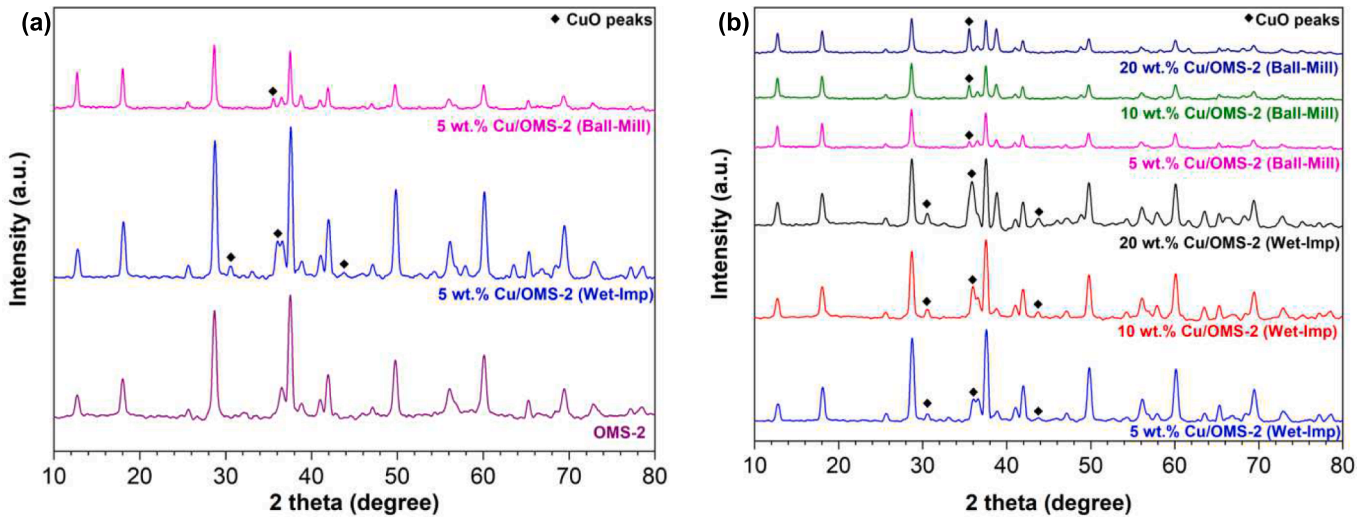

Fig. 1. XRD patterns of **(a)** 5 wt% Cu/OMS-2 catalysts prepared by Wet-Imp and Ball-Mill method; **(b)** 5–20 wt% Cu/OMS-2 catalysts prepared by Wet-Imp and Ball-Mill methods.

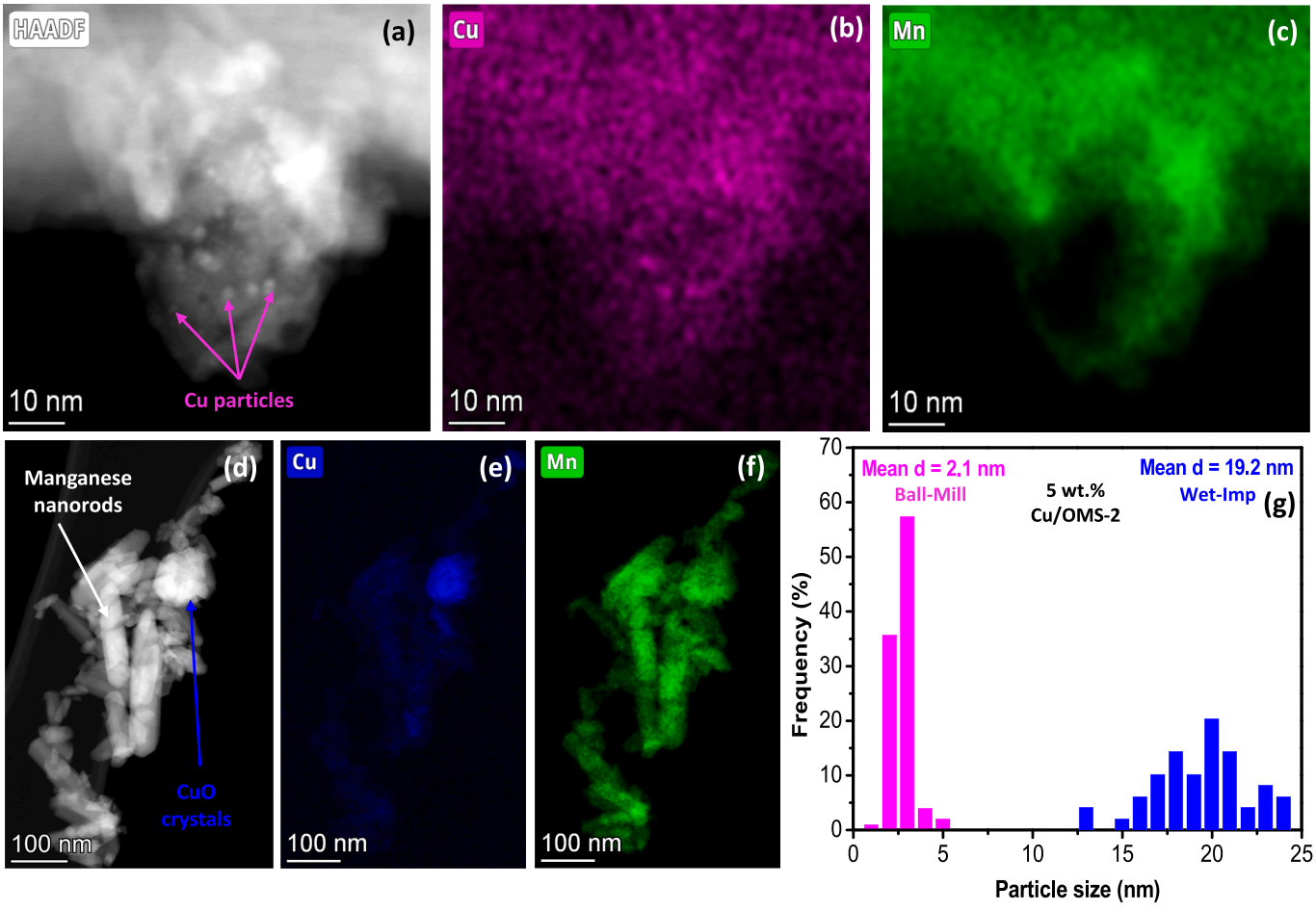

Fig. 2. **(a)** STEM-HAADF image of 5 wt% Cu/OMS-2 (Ball-Mill); **(b)** EDX elemental mapping of Cu distribution for 5 wt% Cu/OMS-2 (Ball-Mill); **(c)** EDX elemental mapping of Mn distribution for 5 wt% Cu/OMS-2 (Ball-Mill); **(d)** STEM-HAADF image of 5 wt% Cu/OMS-2 (Wet-Imp); **(e)** EDX elemental mapping of Cu distribution for 5 wt% Cu/OMS-2 (Wet-Imp); **(f)** EDX elemental mapping of Mn distribution for 5 wt% Cu/OMS-2 (Wet-Img); **(g)** Histogram of CuO particle size distribution of 5 wt% Cu/OMS-2 (Ball-Mill and Wet-Imp).

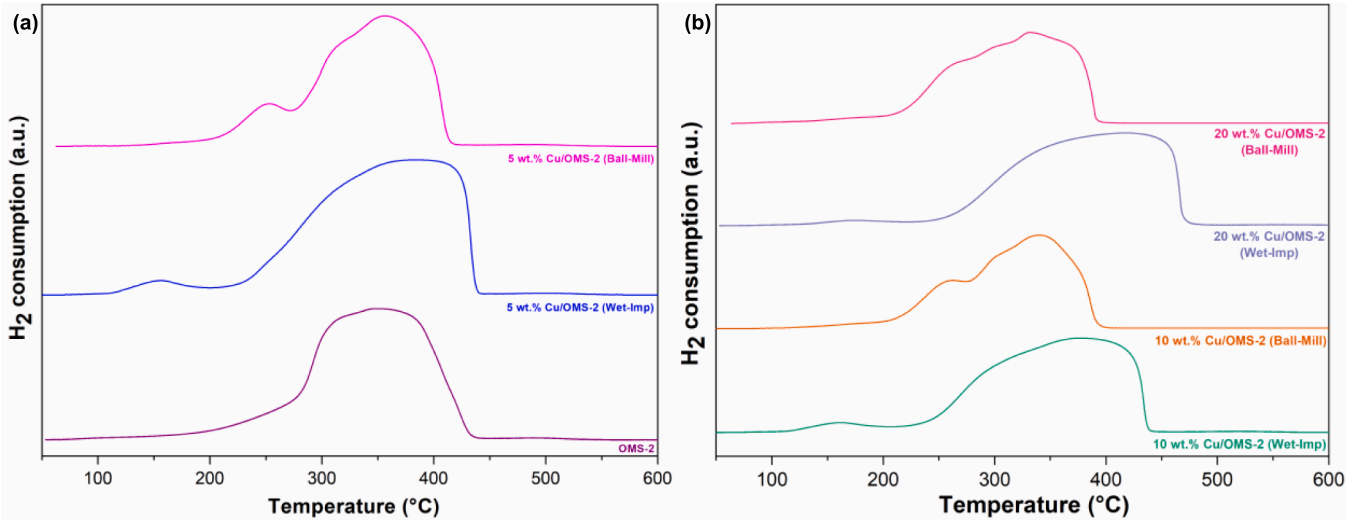

Fig. 3. H_2-TPR profiles of **(a)** 5 wt% Cu/OMS-2 catalysts prepared by Ball-Mill and Wet-Imp methods; **(b)** 10, 20 wt% Cu/OMS-2 catalysts prepared by Ball-Mill and Wet-Imp methods.

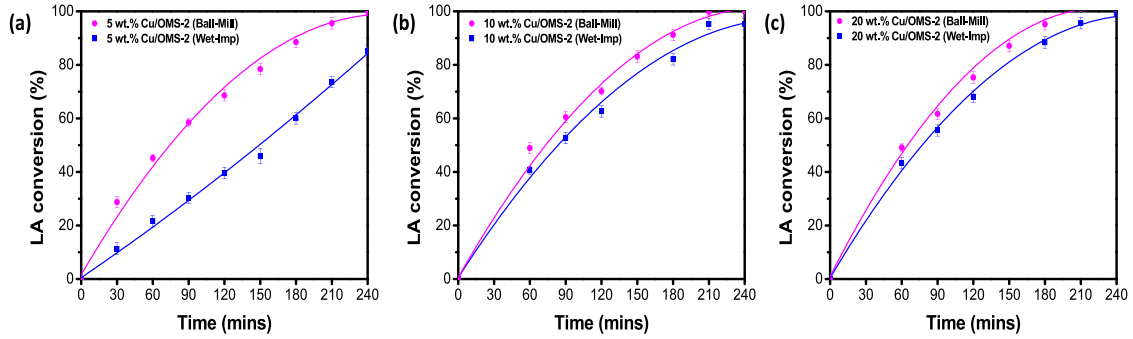

Fig. 4. Reaction time profiles for LA hydrogenation using 5, 10 and 20 wt% Cu/OMS-2 catalysts. Reaction conditions: 1 g LA, 30 ml solvent (1,4-dioxane and water in 3:7 mol ratio), 0.2 g of catalyst at 190 °C temperature and 20 bar H_2 pressure for 240 mins at 1500 rpm.

better Cu/OMS-2 catalysts with superior performance for LA hydrogenation.

3.3. Effect of Cu nanoparticle size on catalyst performance

The effect of Cu nanoparticle size on the catalytic performance for LA hydrogenation to GVL was evaluated by comparing the TOF values based on Cu content, moles of LA converted.moles of $Cu^{-1}.h^{-1}$ (Fig. 5**a**), as well as the intrinsic reaction rate, moles of LA converted.h^{-1} (Fig. 5**b**). The LA hydrogenation TOF values increased for Wet-Imp catalysts in the order 5.9 (20 wt% Cu/OMS-2) < 11.1 (10 wt% Cu/OMS-2) < 11.8 (5 wt % Cu/OMS-2). Here, the TOF values did not show linear dependence on Cu wt.% and similar TOFs were observed for 10 and 5 wt% Cu loading Wet-Img catalysts. However, the Ball-Mill catalysts clearly displayed a linear increase in TOF values for LA hydrogenation, in the order 6.9 (20 wt% Cu/OMS-2) < 13.4 (10 wt% Cu/OMS-2) < 24.7 (5 wt% Cu/OMS-

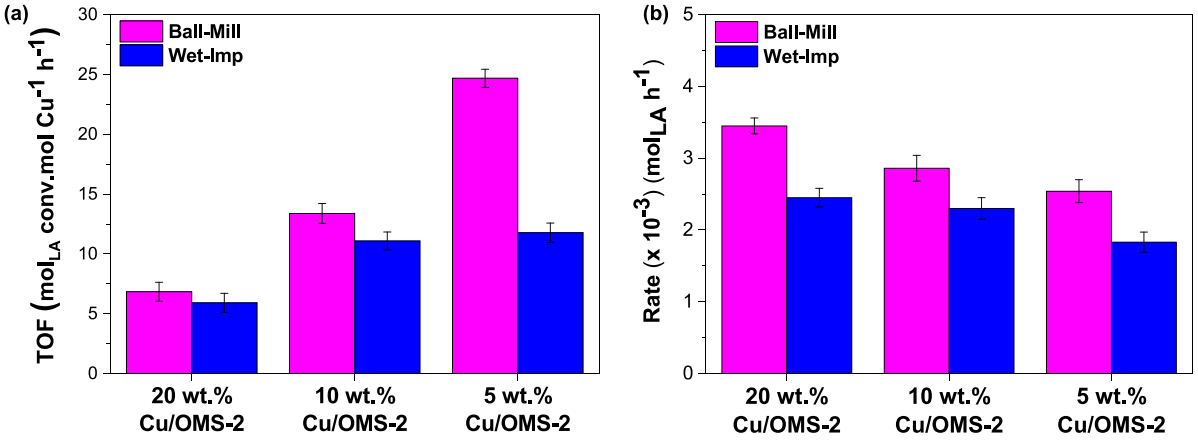

Fig. 5. Relationship between **(a)** TOF for LA conversion for 5, 10, 20 wt% Cu/OMS-2 catalysts; **(b)** Rate of LA conversion for 5, 10 and 20 wt% Cu/OMS-2 catalysts.

2). The maximum TOF value was attained from 5 wt% Cu/OMS-2 (Ball-Mill) with a Cu NP size of 2.1 nm, of all the catalysts. When comparing the catalysts with similar 5 wt% Cu loading prepared by two different methods (5 wt% Cu/OMS-2 (Ball-Mill) and 5 wt% Cu/OMS-2 (Wet-Img)), a notable two-fold enhancement in the TOF value for LA hydrogenation was achieved for the catalysts prepared using ball milling method.

Fig. 5**(b)** shows the comparison of reaction rates arbitrarily calculated at 80 % LA conversion for all catalyst samples, below the equilibrium conversions. A linear increase in LA conversion rates (mol_{LA} h^{-1}) was observed for 5, 10, and 20 wt% Cu/OMS-2 catalysts prepared using ball milling method. The effect was more clearly noticeable for ball-milled catalysts than wet-impregnated catalysts. For all catalysts with similar Cu wt% loadings, catalysts with smaller Cu nanoparticles showed higher reaction rates for LA hydrogenation to GVL. This observation highlights the influence of smaller particle sizes on the rate of LA conversion. The 5 wt% Cu/OMS-2 (Wet-Imp) catalysts showed the lowest LA conversion rate, 1.83 mol_{LA} h^{-1}, while 20 wt% Cu/OMS-2 (Ball-Mill) catalyst showed a two-fold increase with the highest LA conversion rate of 3.45 mol_{LA} h^{-1}.

By decreasing the Cu NP sizes < 5 nm, we were able to achieve higher Cu surface areas and higher Cu metal dispersion on the catalyst surface, resulting in the higher TOF values for LA hydrogenation. In comparison to literature benchmark, for instance, Kon et al. using Pt/HMFI zeolite catalyst, observed the TOF of 33 h^{-1} [11]. Liu et al., using Ni and NiO supported on mesoporous carbon, observed the TOF of 10.8 h^{-1} in LA hydrogenation [66]. Zhang et al. have reported TOF of 7.9 h^{-1} using commercial Ru/C as catalyst. Thus, it is a significant achievement in our study, to get the TOF of 24.7 h^{-1} using 5 wt% Cu/OMS-2 (Ball-Mill) catalyst [67]. Based on literature relating to copper catalysts utilized in the hydrogenation of LA to GVL, our study revealed that the ball-milled catalysts, prepared specifically for this study, exhibit significantly higher TOF. In a separate study, the 5 wt% Cu/γ-Al_2O_3 catalyst showed TOF of 36 h^{-1}, in the reaction at 265 °C [68]. In comparison, Cu catalysts supported on zirconia and ceria yielded TOF values of 5.61 and 0.0365 h^{-1} respectively, in the context of LA hydrogenation to GVL [69,70]. Hengne et al. reported a TON of 9 (equivalent to a calculated TOF of 1.80 h^{-1}) with a 10 mol.% Cu/ZrO_2 catalyst [21]. These examples emphasize the distinctive advantage of our work, as it establishes high TOF with such small copper nanoparticles.

To compare the effect of Cu surface area resulting from varying Cu nanoparticle sizes, we compared the rate of LA conversion (mol_{LA} h^{-1}) to GVL as a function of Cu surface area (◇) for all catalysts with similar Cu loading, prepared using both Wet-Imp and Ball-Mill methods (Fig. 6). For instance, in the case of 20 wt% Cu loading prepared by two different methods (20 wt% Cu/OMS-2 (Wet-Imp) and 20 wt% Cu/OMS-2 (Ball-Mill)), the ball milled catalyst showed higher Cu surface area, which resulted in higher hydrogenation activity in the form of increased reaction rate. The similar behaviour was also observed when corresponding 10 wt% Cu loading Wet-Imp vs Ball-Mill catalysts and 5 wt% Cu loading Wet-Imp vs Ball-Mill catalysts were compared. Furthermore, as the Cu loading increased from 5 to 10 to 20 wt%, the corresponding LA hydrogenation rates also increased due to increased Cu sites.

3.4. Reusability study

The reusability of 5 wt% Cu/OMS-2 catalysts (both Wet-Imp and Ball-Mill) was evaluated for five cycles of LA hydrogenation to GVL. The reusability tests were performed under identical conditions. In a typical

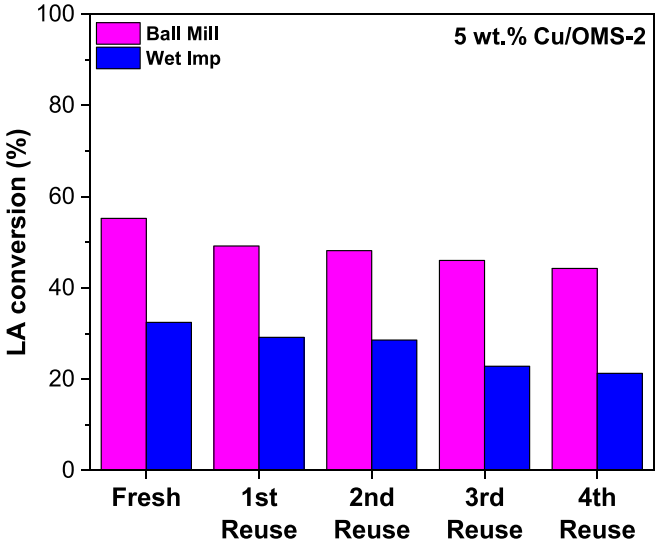

Fig. 7. Effect of catalyst reusability on LA conversion (%) up to five cycles.

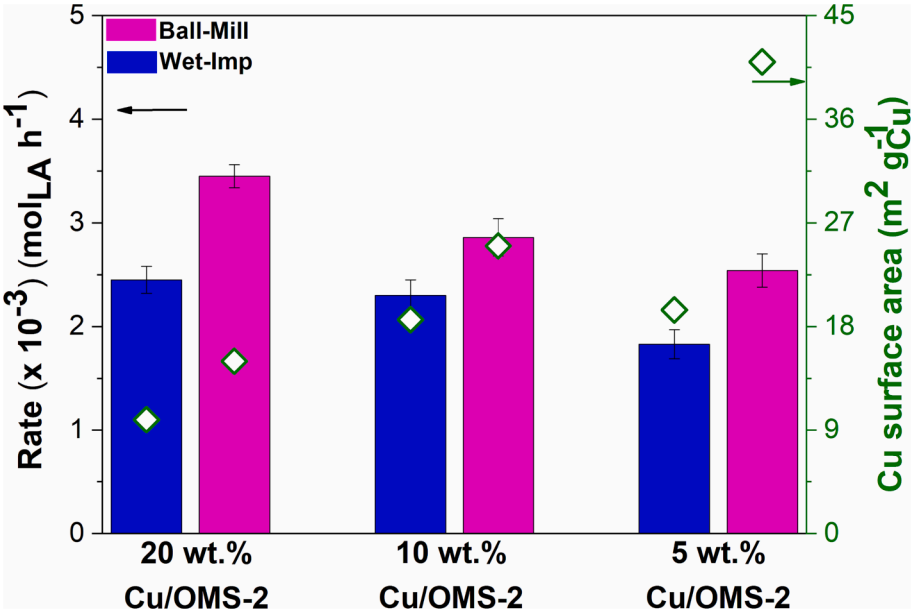

Fig. 6. Corelation between LA conversion rate and Cu surface area in Cu/OMS-2 catalysts.

run, the autoclave reactor was filled with 1 g of LA, a 3:7 mol. ratio of 1,4-dioxane to H_2O mixture and 0.4 g of catalyst. The system was operated at 20 bar H_2 pressure and a temperature of 190 °C for 1 h. After completing the cycle, the catalyst was retrieved, washed, and used for subsequent cycle, without any addition of fresh catalyst for makeup of catalyst loss due to attrition. As shown in Fig. 7, the initial run using fresh 5 wt% Cu/OMS-2 (Ball-Mill) gave 55 % LA conversion, which slightly diminished to 49 % after the first reuse and remained constant until the fourth reuse, with a marginal drop to 44 %. A similar pattern emerged for the 5 wt% Cu/OMS-2 (Wet-Imp) catalyst, which exhibited a 32 % LA conversion during the initial run, followed by reductions to 29 % and eventually reaching a significantly lower LA conversion of 21 % after the fourth recycle. The consistent decline in catalytic activity for both catalysts can be attributed to the presence of loosely bound copper species on the surface that are removed after the initial run, leading to a stabilized conversion of LA. ICP-OES analysis of the spent catalyst revealed a decrease in Cu wt.% from 5.03 to 3.90 (Ball-Mill) and 5.06 to 2.8 (Wet-Imp), corroborating our hypothesis that a small amount of copper leached into the reaction after the initial run.

4. Conclusions

The performance of Cu/OMS-2 catalysts prepared using conventional wet impregnation and mechanochemical methods was evaluated in the LA hydrogenation. The results showed that Ball-Milled catalysts with 20, 10, and 5 wt% Cu/OMS-2 demonstrated higher LA conversion and TOF in comparison to corresponding wet impregnation catalysts. When comparing the catalysts with similar 5 wt% Cu loading prepared by two different methods (5 wt% Cu/OMS-2 (Ball-Mill) and 5 wt% Cu/OMS-2 (Wet-Imp)), a notable two-fold enhancement in the TOF value for LA hydrogenation was achieved for the catalysts prepared using ball milling method. Similarly, in the case of 20 wt% Cu loading prepared by two different methods (20 wt% Cu/OMS-2 (Wet-Imp) and 20 wt% Cu/OMS-2 (Ball-Mill)), the ball milled catalyst showed higher Cu surface area, which resulted in higher hydrogenation activity in the form of increased reaction rate. As the Cu loading (wt.%) increased, the corresponding LA hydrogenation rate also increased due to increased Cu sites. Among the catalysts studied, 5 wt% Cu/OMS-2 displayed the highest LA conversion TOF value of 24.7 mol of LA converted.mol $Cu^{-1}h^{-1}$. Characterization of the catalysts showed differences in Cu NPs size resulting from both the preparation methods. These findings indicated that Cu nanoparticle size is an important catalyst design criteria for improving the catalyst performance.

Declaration of Competing Interest

The authors declare that they have no known competing financial interests or personal relationships that could have appeared to influence the work reported in this paper.

Data availability

Data will be made available on request.

Acknowledgements

The authors gratefully acknowledge the financial support for PhD studentship to N.J.M funded through collaboration initiative between Queen's University Belfast and Tezpur University, India.

References

[1] K. Ralphs, C. Hardacre, S.L. James, Application of heterogeneous catalysts prepared by mechanochemical synthesis, Chem. Soc. Rev. 42 (2013) 7701, https://doi.org/10.1039/c3cs60066a.
[2] M. Klimakow, P. Klobes, A.F. Thünemann, K. Rademann, F. Emmerling, Mechanochemical Synthesis of Metal−Organic Frameworks: A Fast and Facile Approach toward Quantitative Yields and High Specific Surface Areas, Chem. Mater. 22 (2010) 5216–5221, https://doi.org/10.1021/cm1012119.
[3] K. Ralphs, G. Collins, H. Manyar, S.L. James, C. Hardacre, Selective Hydrogenation of Stearic Acid Using Mechanochemically Prepared Titania-Supported Pt and Pt–Re Bimetallic Catalysts, ACS Sustain. Chem. Eng. 10 (2022) 6934–6941, https://doi.org/10.1021/acssuschemeng.1c07595.
[4] J. Barrault, C. Bouchoule, D. Duprez, C. Montassier, G. Pérot, M. Guisnet, Heterogeneous Catalysis and Fine Chemicals, ELSEVIER, 1988. https://www.sciencedirect.com/bookseries/studies-in-surface-science-and-catalysis/vol/41/suppl/C.
[5] A.J. Garcia-Olmo, A. Yepez, A.M. Balu, P. Prinsen, A. Garcia, A. Maziere, C. Len, R. Luque, Activity of continuous flow synthesized Pd-based nanocatalysts in the flow hydroconversion of furfural, Tetrahedron 73 (2017) 5599–5604, https://doi.org/10.1016/j.tet.2017.02.056.
[6] Y. Wang, P. Prinsen, K.S. Triantafyllidis, S.A. Karakoulia, A. Yepez, C. Len, R. Luque, Batch versus Continuous Flow Performance of Supported Mono- and Bimetallic Nickel Catalysts for Catalytic Transfer Hydrogenation of Furfural in Isopropanol, ChemCatChem 10 (2018) 3459–3468, https://doi.org/10.1002/cctc.201800530.
[7] D.M. Alonso, S.G. Wettstein, J.A. Dumesic, Gamma-valerolactone, a sustainable platform molecule derived from lignocellulosic biomass, Green Chem. 15 (2013) 584, https://doi.org/10.1039/c3gc37065h.
[8] Gamma Valerolactone Market Size 2023 Is Projected to Rise at a Positive CAGR by Forecast to 2028, MarketWatch. (2023). https://www.marketwatch.com/press-release/gamma-valerolactone-market-size-2023-is-projected-to-rise-at-a-positive-cagr-by-forecast-to-2028-2023-02-25 (accessed May 16, 2023).
[9] J.-P. Lange, R. Price, P.M. Ayoub, J. Louis, L. Petrus, L. Clarke, H. Gosselink, Valeric Biofuels: A Platform of Cellulosic Transportation Fuels, Angewandte Chemie Int. Ed. 49 (2010) 4479–4483, https://doi.org/10.1002/anie.201000655.
[10] K. Yan, Y. Yang, J. Chai, Y. Lu, Catalytic reactions of gamma-valerolactone: A platform to fuels and value-added chemicals, Appl. Catal. b: Environ. 179 (2015) 292–304, https://doi.org/10.1016/j.apcatb.2015.04.030.
[11] K. Kon, W. Onodera, K. Shimizu, Selective hydrogenation of levulinic acid to valeric acid and valeric biofuels by a Pt/HMFI catalyst, Catal. Sci. Technol. 4 (2014) 3227–3234, https://doi.org/10.1039/C4CY00504J.
[12] Z. Yan, L. Lin, S. Liu, Synthesis of γ-Valerolactone by Hydrogenation of Biomass-derived Levulinic Acid over Ru/C Catalyst, Energy Fuels 23 (2009) 3853–3858, https://doi.org/10.1021/ef900259h.
[13] J.Q. Bond, D.M. Alonso, D. Wang, R.M. West, J.A. Dumesic, Integrated Catalytic Conversion of γ-Valerolactone to Liquid Alkenes for Transportation Fuels, Science 327 (2010) 1110–1114, https://doi.org/10.1126/science.1184362.
[14] V. Fábos, M.Y. Lui, Y.F. Mui, Y.Y. Wong, L.T. Mika, L. Qi, E. Cséfalvay, V. Kovács, T. Szűcs, I.T. Horváth, Use of Gamma-Valerolactone as an Illuminating Liquid and Lighter Fluid, ACS Sustain. Chem. Eng. 3 (2015) 1899–1904, https://doi.org/10.1021/acssuschemeng.5b00465.
[15] J. Zheng, J. Zhu, X. Xu, W. Wang, J. Li, Y. Zhao, K. Tang, Q. Song, X. Qi, D. Kong, Y. Tang, Continuous hydrogenation of ethyl levulinate to γ-valerolactone and 2-methyl tetrahydrofuran over alumina doped Cu/SiO2 catalyst: the potential of commercialization, Sci. Rep. 6 (2016) 28898, https://doi.org/10.1038/srep28898.
[16] L.E. Manzer, Catalytic synthesis of α-methylene-γ-valerolactone: a biomass-derived acrylic monomer, Appl. Catal. a: General. 272 (2004) 249–256, https://doi.org/10.1016/j.apcata.2004.05.048.
[17] I. Obregón, E. Corro, U. Izquierdo, J. Requies, P.L. Arias, Levulinic acid hydrogenolysis on Al2O3-based Ni-Cu bimetallic catalysts, Chin. J. Catal. 35 (2014) 656–662, https://doi.org/10.1016/S1872-2067(14)60051-6.
[18] K. Yan, T. Lafleur, G. Wu, J. Liao, C. Ceng, X. Xie, Highly selective production of value-added γ-valerolactone from biomass-derived levulinic acid using the robust Pd nanoparticles, Appl. Catal. A 468 (2013) 52–58, https://doi.org/10.1016/j.apcata.2013.08.037.
[19] P.P. Upare, J.-M. Lee, Y.K. Hwang, D.W. Hwang, J.-H. Lee, S.B. Halligudi, J.-S. Hwang, J.-S. Chang, Direct Hydrocyclization of Biomass-Derived Levulinic Acid to 2-Methyltetrahydrofuran over Nanocomposite Copper/Silica Catalysts, ChemSusChem 4 (2011) 1749–1752, https://doi.org/10.1002/cssc.201100380.
[20] I. Orlowski, M. Douthwaite, S. Iqbal, J.S. Hayward, T.E. Davies, J.K. Bartley, P. J. Miedziak, J. Hirayama, D.J. Morgan, D.J. Willock, G.J. Hutchings, The hydrogenation of levulinic acid to γ-valerolactone over Cu–ZrO2 catalysts prepared by a pH-gradient methodology, Journal of Energy, Chemistry 36 (2019) 15–24, https://doi.org/10.1016/j.jechem.2019.01.015.
[21] A.M. Hengne, C.V. Rode, Cu–ZrO2 nanocomposite catalyst for selective hydrogenation of levulinic acid and its ester to γ-valerolactone, Green Chem. 14 (2012) 1064, https://doi.org/10.1039/c2gc16558a.
[22] Q. Xu, X. Li, T. Pan, C. Yu, J. Deng, Q. Guo, Y. Fu, Supported copper catalysts for highly efficient hydrogenation of biomass-derived levulinic acid and γ-valerolactone, Green Chem. 18 (2016) 1287–1294, https://doi.org/10.1039/C5GC01454A.
[23] D.R. Jones, S. Iqbal, S. Ishikawa, C. Reece, L.M. Thomas, P.J. Miedziak, D. J. Morgan, J.K. Edwards, J.K. Bartley, D.J. Willock, G.J. Hutchings, The conversion of levulinic acid into γ-valerolactone using Cu–ZrO2 catalysts,, Catal. Sci. Technol. 6 (2016) 6022–6030, https://doi.org/10.1039/C6CY00382F.
[24] S. Ishikawa, D.R. Jones, S. Iqbal, C. Reece, D.J. Morgan, D.J. Willock, P. J. Miedziak, J.K. Bartley, J.K. Edwards, T. Murayama, W. Ueda, G.J. Hutchings, Identification of the catalytically active component of Cu–Zr–O catalyst for the hydrogenation of levulinic acid to γ-valerolactone, Green Chem. 19 (2017) 225–236, https://doi.org/10.1039/C6GC02598F.

[25] D. He, Q. He, P. Jiang, G. Zhou, R. Hu, W. Fu, Novel Cu/Al2O3-ZrO2 composite for selective hydrogenation of levulinic acid to γ-valerolactone, Catal. Commun. 125 (2019) 82–86, https://doi.org/10.1016/j.catcom.2019.03.029.

[26] M. Popova, I. Trendafilova, M. Oykova, Y. Mitrev, P. Shestakova, M.R. Mihályi, Á. Szegedi, Hydrodeoxygenation of Levulinic Acid to γ-Valerolactone over Mesoporous Silica-Supported Cu-Ni Composite Catalysts, Molecules 27 (2022) 5383, https://doi.org/10.3390/molecules27175383.

[27] Y. Li, X. Lan, B. Liu, T. Wang, Synthesis of γ-valerolactone from ethyl levulinate hydrogenation and ethyl 4-hydroxypentanoate lactonization over supported Cu-Ni bimetallic, bifunctional catalysts, J. Ind. Eng. Chem. 107 (2022) 215–223, https://doi.org/10.1016/j.jiec.2021.11.048.

[28] J.-F. Li, L. Zhao, J. Li, M. Li, C.-L. Liu, R.-Z. Yang, W.-S. Dong, Highly selective synthesis of γ-valerolactone from levulinic acid at mild conditions catalyzed by boron oxide doped Cu/ZrO2 catalysts, Appl. Catal. A 587 (2019), 117244, https://doi.org/10.1016/j.apcata.2019.117244.

[29] J. Yuan, S.-S. Li, L. Yu, Y.-M. Liu, Y. Cao, H.-Y. He, K.-N. Fan, Copper-based catalysts for the efficient conversion of carbohydrate biomass into γ-valerolactone in the absence of externally added hydrogen, Energ. Environ. Sci. 6 (2013) 3308–3313, https://doi.org/10.1039/C3EE40857D.

[30] N. Yu, H. Lu, W. Yang, Y. Zheng, Q. Hu, Y. Liu, K. Wu, B. Liang, Transfer hydrogenation of levulinic acid to γ-valerolactone over acid site-modified CuNi alloy, Biomass Conv. Bioref. (2022), https://doi.org/10.1007/s13399-022-02887-2.

[31] B. Cai, X.-C. Zhou, Y.-C. Miao, J.-Y. Luo, H. Pan, Y.-B. Huang, Enhanced Catalytic Transfer Hydrogenation of Ethyl Levulinate to γ-Valerolactone over a Robust Cu–Ni Bimetallic Catalyst, ACS Sustain. Chem. Eng. 5 (2017) 1322–1331, https://doi.org/10.1021/acssuschemeng.6b01677.

[32] C. Fang, S. Kuboon, P. Khemthong, T. Butburee, P. Chakthranont, V. Itthibenchapong, P. Kasamechonchung, T. Witoon, K. Faungnawakij, Highly dispersed NiCu nanoparticles on SBA-15 for selective hydrogenation of methyl levulinate to γ-valerolactone, Int. J. Hydrogen Energy 45 (2020) 24054–24065, https://doi.org/10.1016/j.ijhydene.2019.03.272.

[33] L. Takacs, The historical development of mechanochemistry, Chem. Soc. Rev. 42 (2013) 7649, https://doi.org/10.1039/c2cs35442j.

[34] K. Ralphs, S. Chansai, C. Hardacre, R. Burch, S.F.R. Taylor, S.L. James, Mechanochemical preparation of Ag catalysts for the n-octane-SCR de-NOx reaction: Structural and reactivity effects, Catal. Today 246 (2015) 198–206, https://doi.org/10.1016/j.cattod.2014.10.027.

[35] U. Kamolphop, Sarah.F.R. Taylor, J.P. Breen, R. Burch, J.J. Delgado, S. Chansai, C. Hardacre, S. Hengrasmee, S.L. James, Low-Temperature Selective Catalytic Reduction (SCR) of NOx with n-Octane Using Solvent-Free Mechanochemically Prepared Ag/Al_2O_3 Catalysts, ACS Catal. 1 (2011) 1257–1262. Doi: 10.1021/cs200326m.

[36] T.J. Clarke, T.E. Davies, S.A. Kondrat, S.H. Taylor, Mechanochemical synthesis of copper manganese oxide for the ambient temperature oxidation of carbon monoxide, Appl Catal B 165 (2015) 222–231, https://doi.org/10.1016/j.apcatb.2014.09.070.

[37] C. Coney, C. Hardacre, K. Morgan, N. Artioli, A.P.E. York, P. Millington, A. Kolpin, A. Goguet, Investigation of the oxygen storage capacity behaviour of three way catalysts using spatio-temporal analysis, Appl Catal B 258 (2019), 117918, https://doi.org/10.1016/j.apcatb.2019.117918.

[38] G.D. Yadav, H.G. Manyar, Synthesis of a Novel Redox Material UDCaT-3: An Efficient and Versatile Catalyst for Selective Oxidation, Hydroxylation and Hydrogenation Reactions, Adv. Synth. Catal. 350 (2008) 2286–2294, https://doi.org/10.1002/adsc.200800313.

[39] T. Jakubek, K. Ralphs, A. Kotarba, H. Manyar, Nanostructured Potassium-Manganese Oxides Decorated with Pd Nanoparticles as Efficient Catalysts for Low-Temperature Soot Oxidation, Catal. Lett. 149 (2019) 100–106, https://doi.org/10.1007/s10562-018-2585-z.

[40] T. Jakubek, C. Hudy, J. Gryboś, H. Manyar, A. Kotarba, Thermal Transformation of Birnessite (OL) Towards Highly Active Cryptomelane (OMS-2) Catalyst for Soot Oxidation, Catal. Lett. 149 (2019) 2218–2225, https://doi.org/10.1007/s10562-019-02828-1.

[41] T.G.A. Youngs, H. Manyar, D.T. Bowron, L.F. Gladden, C. Hardacre, Probing chemistry and kinetics of reactions in heterogeneous catalysts, Chem. Sci. 4 (2013) 3484, https://doi.org/10.1039/c3sc51477c.

[42] H.G. Manyar, R. Morgan, K. Morgan, B. Yang, P. Hu, J. Szlachetko, J. Sá, C. Hardacre, High energy resolution fluorescence detection XANES – an in situ method to study the interaction of adsorbed molecules with metal catalysts in the liquid phase, Cat. Sci. Technol. 3 (2013) 1497, https://doi.org/10.1039/c3cy00031a.

[43] X. Chen, Z. Wang, H. Daly, R. Morgan, H. Manyar, C. Byrne, A.S. Walton, S.F. R. Taylor, M. Smith, R. Burch, P. Hu, C. Hardacre, Hydrogenation of benzoic acid to benzyl alcohol over Pt/SnO2, Appl. Catal. A 593 (2020), 117420, https://doi.org/10.1016/j.apcata.2020.117420.

[44] M.T. Rahman, S. Wharry, M. Smyth, H. Manyar, T.S. Moody, FAST Hydrogenations as a Continuous Platform for Green Aromatic Nitroreductions, Synlett 31 (2020) 581–586, https://doi.org/10.1055/s-0037-1610751.

[45] R. O'Donnell, K. Ralphs, M. Grolleau, H. Manyar, N. Artioli, Doping Manganese Oxides with Ceria and Ceria Zirconia Using a One-Pot Sol-Gel Method for Low Temperature Diesel Oxidation Catalysts, Top. Catal. 63 (2020) 351–362, https://doi.org/10.1007/s11244-020-01250-x.

[46] H.G. Manyar, B. Yang, H. Daly, H. Moor, S. McMonagle, Y. Tao, G.D. Yadav, A. Goguet, P. Hu, C. Hardacre, Selective Hydrogenation of α, β-Unsaturated Aldehydes and Ketones using Novel Manganese Oxide and Platinum Supported on Manganese Oxide Octahedral Molecular Sieves as Catalysts, ChemCatChem 5 (2013) 506–512, https://doi.org/10.1002/cctc.201200447.

[47] N.J. Mazumdar, G. Deshmukh, A. Rovea, P. Kumar, M. Arredondo-Arechavala, H. Manyar, Insights into selective hydrogenation of levulinic acid using copper on manganese oxide octahedral molecular sieves, R. Soc. Open Sci. 9 (2022), 220078, https://doi.org/10.1098/rsos.220078.

[48] J. Salisu, N. Gao, C. Quan, J. Yanik, N. Artioli, Co-gasification of rice husk and plastic in the presence of CaO using a novel ANN model-incorporated Aspen plus simulation, J. Energy Inst. 108 (2023), 101239, https://doi.org/10.1016/j.joei.2023.101239.

[49] C. Quan, G. Zhang, N. Gao, S. Su, N. Artioli, D. Feng, Behavior Study of Migration and Transformation of Heavy Metals during Oily Sludge Pyrolysis, Energy Fuels 36 (2022) 8311–8322, https://doi.org/10.1021/acs.energyfuels.2c01283.

[50] E.L. Byrne, R. O'Donnell, M. Gilmore, N. Artioli, J.D. Holbrey, M. Swadźba-Kwaśny, Hydrophobic functional liquids based on trioctylphosphine oxide (TOPO) and carboxylic acids, PCCP 22 (2020) 24744–24763, https://doi.org/10.1039/D0CP02605K.

[51] L. Castoldi, R. Matarrese, L. Kubiak, M. Daturi, N. Artioli, S. Pompa, L. Lietti, In-depth insights into N2O formation over Rh- and Pt-based LNT catalysts, Catal. Today 320 (2019) 141–151, https://doi.org/10.1016/j.cattod.2018.01.026.

[52] M.T. Yilleng, E.C. Gimba, G.I. Ndukwe, I.M. Bugaje, D.W. Rooney, H.G. Manyar, Batch to continuous photocatalytic degradation of phenol using TiO2 and Au-Pd nanoparticles supported on TiO2, Journal of Environmental, Chem. Eng. 6 (2018) 6382–6389, https://doi.org/10.1016/j.jece.2018.09.048.

[53] J. Ethiraj, D. Wagh, H. Manyar, Advances in Upgrading Biomass to Biofuels and Oxygenated Fuel Additives Using Metal Oxide Catalysts, Energy Fuels 36 (2022) 1189–1204, https://doi.org/10.1021/acs.energyfuels.1c03346.

[54] K. Pandit, C. Jeffrey, J. Keogh, M.S. Tiwari, N. Artioli, H.G. Manyar, Techno-Economic Assessment and Sensitivity Analysis of Glycerol Valorization to Biofuel Additives via Esterification, Ind. Eng. Chem. Res. 62 (2023) 9201–9210, https://doi.org/10.1021/acs.iecr.3c00964.

[55] S. Sithambaram, E.K. Nyutu, S.L. Suib, OMS-2 catalyzed oxidation of tetralin: A comparative study of microwave and conventional heating under open vessel conditions, Appl. Catal. A 348 (2008) 214–220, https://doi.org/10.1016/j.apcata.2008.06.046.

[56] D. Mardiansyah, T. Badloe, K. Triyana, M.Q. Mehmood, N. Raeis-Hosseini, Y. Lee, H. Sabarman, K. Kim, J. Rho, Effect of temperature on the oxidation of Cu nanowires and development of an easy to produce, oxidation-resistant transparent conducting electrode using a PEDOT:PSS coating, Sci. Rep. 8 (2018) 10639, https://doi.org/10.1038/s41598-018-28744-9.

[57] D. Zhu, L. Wang, W. Yu, H. Xie, Intriguingly high thermal conductivity increment for CuO nanowires contained nanofluids with low viscosity, Sci. Rep. 8 (2018) 5282, https://doi.org/10.1038/s41598-018-23174-z.

[58] X. Yang, H. Chen, Q. Meng, H. Zheng, Y. Zhu, Y.W. Li, Insights into influence of nanoparticle size and metal–support interactions of Cu/ZnO catalysts on activity for furfural hydrogenation, Catal Sci. Technol. 7 (2017) 5625–5634, https://doi.org/10.1039/C7CY01284E.

[59] J.Y. Kim, J.A. Rodriguez, J.C. Hanson, A.I. Frenkel, P.L. Lee, Reduction of CuO and Cu2O with H2: H Embedding and Kinetic Effects in the Formation of Suboxides, J. Am. Chem. Soc. 125 (2003) 10684–10692, https://doi.org/10.1021/ja0301673.

[60] F. Dong, Y. Zhu, G. Ding, J. Cui, X. Li, Y. Li, One-step Conversion of Furfural into 2-Methyltetrahydrofuran under Mild Conditions, ChemSusChem 8 (2015) 1534–1537, https://doi.org/10.1002/cssc.201500178.

[61] H. Yen, Y. Seo, S. Kaliaguine, F. Kleitz, Tailored Mesostructured Copper/Ceria Catalysts with Enhanced Performance for Preferential Oxidation of CO at Low Temperature, Angew. Chem. Int. Ed. 51 (2012) 12032–12035, https://doi.org/10.1002/anie.201206505.

[62] Z. Huang, F. Cui, J. Xue, J. Zuo, J. Chen, C. Xia, Cu/SiO2 catalysts prepared by hom- and heterogeneous deposition–precipitation methods: Texture, structure, and catalytic performance in the hydrogenolysis of glycerol to 1,2-propanediol, Catal. Today 183 (2012) 42–51, https://doi.org/10.1016/j.cattod.2011.08.038.

[63] Y. Zhao, A. Jalal, A. Uzun, Interplay between Copper Nanoparticle Size and Oxygen Vacancy on Mg-Doped Ceria Controls Partial Hydrogenation Performance and Stability, ACS Catal. 11 (2021) 8116–8131, https://doi.org/10.1021/acscatal.1c01471.

[64] J. Zhang, X. Meng, C. Yu, G. Chen, P. Zhao, Heterogeneous Cu/OMS-2 as an efficient catalyst for the synthesis of tetrasubstituted 1,4-enediones and 4H-pyrido [1,2-a]-pyrimidin-4-ones, RSC Adv. 5 (2015) 87221–87227, https://doi.org/10.1039/C5RA17351E.

[65] I.J. McManus, H. Daly, H.G. Manyar, S.F.R. Taylor, J.M. Thompson, C. Hardacre, Selective hydrogenation of halogenated arenes using porous manganese oxide (OMS-2) and platinum supported OMS-2 catalysts, Faraday Discuss. 188 (2016) 451–466, https://doi.org/10.1039/C5FD00227C.

[66] X. Liu, Z. Li, Efficient transfer hydrogenation of levulinic acid (LA) to γ-valerolactone (GVL) over Ni/NiO–MC (MC = mesoporous carbon), Sustainable, Energy Fuels 5 (2021) 3312–3320, https://doi.org/10.1039/D1SE00228G.

[67] K. Zhang, Q. Meng, H. Wu, T. Yuan, S. Han, J. Zhai, B. Zheng, C. Xu, W. Wu, M. He, B. Han, Levulinic acid hydrogenation to γ-valerolactone over single Ru atoms on a TiO_2 @nitrogen doped carbon support, Green Chem. 23 (2021) 1621–1627, https://doi.org/10.1039/D0GC04108D.

[68] B. Putrakumar, N. Nagaraju, V.P. Kumar, K.V.R. Chary, Hydrogenation of levulinic acid to γ-valerolactone over copper catalysts supported on γ-Al2O3, Catal. Today 250 (2015) 209–217, https://doi.org/10.1016/j.cattod.2014.07.014.
[69] P. Balla, V. Perupogu, P.K. Vanama, V.C. Komandur, Hydrogenation of biomass-derived levulinic acid to γ-valerolactone over copper catalysts supported on ZrO2, J. Chem. Technol. Biotechnol. 91 (2016) 769–776, https://doi.org/10.1002/jctb.4643.
[70] H. Mitta, V. Perupogu, R. Boddula, S.R. Ginjupalli, A.M.A. Inamuddin, Enhanced production of γ-valerolactone from levulinic acid hydrogenation-cyclization over ZrxCe1-xO2 based Cu catalysts, Int. J. Hydrogen Energy 45 (2020) 26445–26457, https://doi.org/10.1016/j.ijhydene.2019.11.149.